TS please include this in the header *Vol 9(13), DOI: 10.17485/ijst/2016/v9i13/90585, April 2016*
ISSN (Print) : 0974-6846
ISSN (Online) : 0974-5645

Experimental Investigations and Prediction on MRR and SR of Some Non Ferrous Alloys in AWJM Using ANFIS

K. S. Jai Aultrin[1] and M. Dev Anand[2]*

[1]Noorul Islam Centre for Higher Education, Kumaracoil - 629180, Thuckalay, Tamil Nadu, India; josephpaulpv@gmail.com
[2]Department of Mechanical Engineering, Noorul Islam Centre for Higher Education, Kumaracoil - 629180, Thuckalay, Tamil Nadu, India; anandpmt@gmail.com

Abstract

Background/Objectives: Last decades have witnessed a rapid growth in the development of harder, difficult and complexity to machine metals and alloys. Abrasive Water Jet Machining (AWJM) is one of the recently developed nontraditional mechanical type hybrid machining processes in processing various kinds of hard-to-cut materials. It is an economical method for heat sensitive materials that cannot be machined by processes that produce heat while machining. Machining parameters play the lead role in determining the machine economics and quality of machining. This paper investigates the prediction of MRR and SR on Aluminum, Copper and Lead alloys using the combination of Artificial Neural Network (ANN) and Fuzzy Logic (FL). **Methods/Statistical Analysis:** In this study, the consequence of different AWJM process parameters on Material Removal Rate (MRR) and Surface Roughness (SR) of three nonferrous alloys namely Aluminum, Copper and Lead which are machined by AWJM was experimentally performed and analyzed. According to Response Surface Methodology (RSM) design, different experiments were conducted with the combination of input parameters on these alloys. **Findings:** A combinational method called as Adaptive Neuro Fuzzy Inference System provides effective knowledge based training to process parameters, to make its enhancement of process performance.

Keywords: Abrasive Water Jet Machining, Adaptive Neuro Fuzzy Inference System, Material Removal Rate, Response Surface Methodology, Surface Roughness

1. Introduction and Review of Literature

AWJM is the recently developed hybrid processes. This technique is suitable for machining of brittle materials similar to glass, ceramics and stones as well as for composite materials, ferrous and non-ferrous materials. From the literature review of Adel[1] in 2011 an elastic-plastic erosion model was implemented to build up an Abrasive Water Jet (AWJ) model for machining brittle materials. C. Ma, R.T. Deam[2] in 2006 investigated that kerf geometry have been measured by the use of an optical microscope. With these measurements, an empirical correlation for kerf profile shape under various traverse speed have been developed that fits the kerf shape well[2]. Computational Fluid Dynamics (CFD) models for ultrahigh velocity water jets and AWJs are established by the use of Fluent6 flow solver[3]. Performed micro-EDM and hybrid process of micro-wire electrical discharge grinding to assess the inaccuracies while machining. They examined the MRR, SR and TWR results by ANN and ANFIS and showed that the ANFIS model is better when compared with ANN[4]. Performed ANFIS model for SR on D5 tool steel in WEDM process and examined the metallographic properties[5]. Jang observed from that Artificial Intelligence (AI) techniques comprising of ANN, FL and Taguchi based fuzzy systems have wide applications in modeling of WEDM process parameters. In this modeled the process parameters with ANFIS which combines the ANN adaptive capability and FL qualitative

*Author for correspondence

approach[6]. In their study modeled for SR and white layer thickness after WEDM by using ANFIS by considering pulse duration, dielectric flushing pressure, wire feed rate and open circuit voltage as parameters[7]. In his study considered the prediction of SR by ANFIS which is the output parameter and feed rate, current, and pulse on time are chosen as the independent variables in WEDM process[8].

2. Experimental Work

2.1 Material

The three materials chosen for this study are Aluminium6061alloy, Copper Iron alloy and Lead Tin alloy. Aluminium 6061 alloy is a precipitation hardening Aluminium alloy which is available in several forms such as tube, ingot, ribbon, wire, foil, bar, pipe and rod. The important factor in selecting Aluminum 6061 alloy is their high strength to weight ratio, appearance, and their nonmagnetic properties. Some of the applications of Aluminium 6061 alloy include marine fittings, aerospace maintenance, transport, bicycle frames, brake components, valves couplings etc.

Copper and its alloys was used as a building material, a conductor of heat and electricity, and as a component of various metal alloys. Because of its high electrical conductivity, huge quantity of Copper are applied in electrical industry for wire. As Copper was resistant to corrosion due to moisture, it's widely used and applied in jewelry, coins, and pipes. As Copper is too soft for applications, it is integrated in various alloys. This alloy is available as wire, sheet, shot, bar, ingot, ribbon, and foil. It has superb corrosion resistance for atmospheric conditions.

Lead Tin alloy, an American element is available in several forms such as tube, ingot, ribbon, wire, foil, bar, pipe and rod. The important factor in selecting Lead Tin alloy is their high strength to weight ratio, their resistance to corrosion by many chemicals, their high thermal and electrical conductivity, non-toxicity, reflectivity, and appearance, and their ease of formability and machinability and nonmagnetic properties. Some of the applications of Lead Tin alloy include marine fittings, aerospace maintenance, transport, bicycle frames, brake components, valves couplings etc. The dimension of these alloys used for this study is 150mm x 50mm x 50mm. shown in Figure 1.

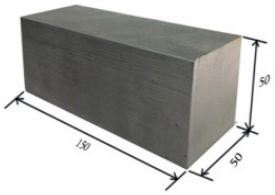

(a)

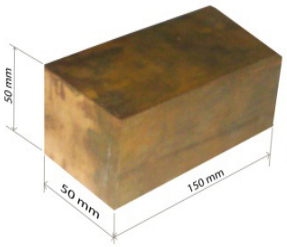

(b)

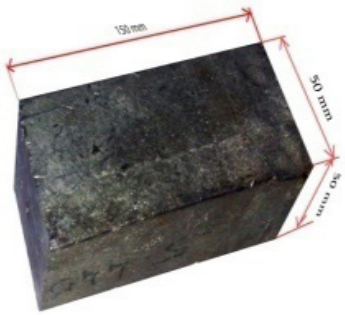

(c)

Figure 1. Non Ferrous Alloys. (a) Aluminium 6061Alloy. (b) Copper Iron. (c) Lead Tin Alloy.

2.2 Response Surface Methodology

RSM is a set of mathematical and statistical techniques[9] which are useful for modeling and investigation of problems. In the present study five process parameters are chosen and varied in three levels as shown in Table 1.

Based on response surface methodology, Box-Behnken design 46 sets of experimental design were selected.

Table 1. Levels of parameters used in experiment

Levels	Water Pressure (P) Bar	Abrasive Flow Rate (mf) Kg/m3	Orifice Diameter (do) mm	Focusing Nozzle Diameter (df) mm	Stand Off Distance (s) mm
Low	3400	0.40	0.30	0.90	1
Intermediate	3600	0.55	0.33	0.99	2
High	3800	0.70	0.35	1.05	3

2.3 Experimentation

The machine used to cut all the three nonferrous alloys was the AWJM machine is set with KMT Ultrahigh Pressure Pump with the designed pressure of 4000bar; gravity feed type of abrasive hopper, an abrasive feeder system, a pneumatically controlled valve and a work piece table[10,11]. The controller fixed in the control stand is used to adjust the SOD for different experiments. The abrasive water jet machine is programmed using numerical control code is to change the transverse speed and manage the supplement of abrasives. After the water is pumped at very high pressures resulting in high velocity of water jet of 1000m/s as it comes out of focusing nozzle cuts the materials of the desired size and shape. The KMT abrasive water jet cutting machine is shown in Figure 2.

For performing the experiments it has to design the combination of input parameters for each experiment and how many experiments has to be done. For this purpose using Minitab software according to the Box-Behnken design of RSM, with five input parameters, 46 experimental designs is selected and performed experimentally and machining time is observed for all experiments as shown in Table 2. The MRR is calculated by the formula;

$$MRR = (m_f - m_i)/t$$

Where, m_f = mass of the material after machining, m_i = mass of the material before machining and t = Machining Time.

The SR for the machined Alloys is measured using portable surface roughness tester.

The mathematical model for the experimental data by cutting all the three nonferrous alloys using AWJM for MRR and SR is developed using linear regression analysis through Minitab software. The developed regression equations are given below.

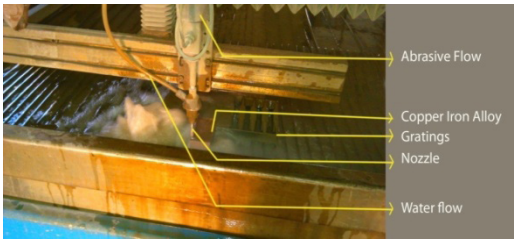

Figure 2. Experimental Setup of AWJM with Mixing Chamber.

For Aluminium:

MRR = 195.719 - 0.360226A + 99.1877B + 1516.21C + 364.430D - 6.05121E + 6.23441e ^{05}A*A - 1.34839B*B - 802.864C*C - 82.6080D*D - 0.410467E*E + 0.00196733A*B - 0.102446A*C - 0.0265738A*D + 0.000769113A*E - 300.422B*C + 15.6465B*D + 0.470717B*E - 438.266C*D - 18.4785C*E + 10.3697D*E

SR = 179.473 - 0.0589755A + 6.28678B - 132.385C - 94.7475D + 1.76521E + 7.04007e^{-06}A*A - 2.89173B*B + 32.5335C*C + 19.3324D*D + 0.0255693E*E + 0.00175000A*B + 0.00161011A*C + 0.00528029A*D - 7.12500e^{-04}A*E - 19.9095B*C – 3.55958B*D -0.216667B*E + 113.234C*D - 0.0302120C*E + 1.16942D*E

For Copper:

MRR = 3807.07 - 0.865684A - 1541.90B - 13291.1C - 620.554D + 717.689E + 0.000235908A*A - 678.682B*B + 16370.4C*C + 619.730D*D + 26.3263 E*E + 0.482583A*B + 2.17099A*C + 0.222252A*D - 0.219850A*E - 954.417B*C + 572.784B*D + 174.917B*E - 5426.25C*D + 110.636C*E + 171.187D*E

SR= 31.3516 + 0.00233958A - 31.1430B - 137.754C - 6.56011D + 7.28615E + 5.14367e^{-07}A*A - 1.21594B*B + 220.213C*C + 9.75236D*D + 0.0385801E*E + 0.00484167A*B - 0.00887783A*C - 0.00505543A*D

Table 2. Scheduling Matrix of the Experiments with the Optimal Model Data

Input Parameters					Output Parameters					
Pressure (Bar)	Abrasive Flow Rate (Kg/min)	Orifice Diameter (mm)	Focusing Tube Diameter (mm)	Stand Off Distance (mm)	MRR mm3/min Al	SR µm Al	MRR mm3/ min Cu	SR µm Cu	MRR mm3/min Pb	SR µm Pb
3400	0.55	0.33	0.99	3	48.6111	3.57	897.80	3.62	1709.00	2.450
3600	0.55	0.33	0.9	1	53.6399	2.08	1000.03	1.63	2014.86	1.415
3600	0.55	0.3	1.05	2	51.8519	2.21	961.93	2.24	1970.09	1.624
3600	0.55	0.33	0.9	3	50.8352	2.55	918.21	3.09	1916.85	2.200
3800	0.55	0.33	0.9	2	62.2222	1.90	1043.96	1.767	2182.26	0.788
3600	0.55	0.33	0.99	2	51.8519	2.19	928.76	2.228	1997.84	1.609
3400	0.4	0.33	0.99	2	45.7516	3.20	762.29	3.309	1688.65	2.109
3600	0.7	0.35	0.99	2	53.6399	1.80	985.39	2.19	1997.84	1.520
3800	0.55	0.33	0.99	3	61.2423	2.07	987.80	1.901	2085.98	1.201
3800	0.55	0.3	0.99	2	62.2222	2.05	1025.41	1.66	2149.19	0.801
3600	0.55	0.33	0.99	3	51.1696	2.54	907.89	2.77	1896.34	2.100
3400	0.55	0.33	1.05	2	47.7164	3.08	800.02	2.991	1746.88	1.905
3600	0.4	0.33	0.99	1	50.1792	1.99	920.30	1.989	1943.11	1.887
3600	0.55	0.33	0.99	2	52.9101	2.17	922.40	2.224	2009.16	1.571
3600	0.55	0.35	0.9	2	54.3901	2.08	948.38	2.43	1948.44	1.530
3600	0.55	0.3	0.9	2	51.8519	2.79	950.62	2.32	2003.48	1.709
3400	0.55	0.33	0.9	2	48.6111	3.30	817.84	2.83	1751.19	1.900
3600	0.55	0.33	0.99	2	52.9101	2.19	897.80	2.29	2003.48	1.566
3600	0.4	0.3	0.99	2	47.7164	2.36	827.89	2.589	1842.16	1.910
3400	0.55	0.35	0.99	2	48.3092	2.95	814.54	3.19	1751.19	1.899
3800	0.4	0.33	0.99	2	58.4785	1.89	961.93	1.799	2136.25	1.211
3600	0.7	0.33	0.99	3	54.7731	2.25	997.56	2.357	1891.29	1.999
3600	0.7	0.33	0.99	1	56.3607	1.68	987.80	1.50	2055.75	1.431
3600	0.4	0.35	0.99	2	49.2264	2.29	846.98	2.70	1866.40	2.013
3600	0.4	0.33	0.9	2	48.9168	2.36	863.27	2.79	1842.16	1.945
3600	0.55	0.35	0.99	3	51.1696	2.50	928.76	3.03	1916.85	2.008
3600	0.7	0.33	0.9	2	55.9552	2.14	973.52	1.85	1970.09	1.500
3400	0.55	0.33	0.99	1	49.2264	2.65	792.18	2.24	1800.08	1.789
3600	0.7	0.3	0.99	2	56.7721	2.18	973.52	1.734	1937.80	1.699
3600	0.55	0.33	1.05	1	50.8352	1.90	957.37	2.00	2049.81	1.707
3600	0.55	0.3	0.99	1	51.8519	1.99	990.22	1.66	2009.16	1.500
3800	0.7	0.33	0.99	2	64.8148	1.70	1100.85	1.407	2142.69	0.620
3600	0.4	0.33	1.05	2	48.6111	2.40	824.51	2.47	1866.40	1.934
3600	0.55	0.3	0.99	3	52.1999	2.68	939.56	2.80	1916.84	2.309
3600	0.55	0.33	0.99	2	52.9101	2.20	922.40	2.201	2014.86	1.597
3800	0.55	0.33	1.05	2	59.8291	1.99	1035.93	1.564	2162.30	0.800

Table 2. Scheduling Matrix of the Experiments with the Optimal Model Data

Input Parameters					Output Parameters					
Pressure (Bar)	Abrasive Flow Rate (Kg/min)	Orifice Diameter (mm)	Focusing Tube Diameter (mm)	Stand Off Distance (mm)	MRR mm3/min Al	SR µm Al	MRR mm3/ min Cu	SR µm Cu	MRR mm3/min Pb	SR µm Pb
3400	0.7	0.33	0.99	2	51.8519	2.80	831.30	2.456	1800.08	1.900
3600	0.55	0.35	1.05	2	51.1696	2.34	907.89	2.56	2020.60	1.704
3400	0.55	0.3	0.99	2	48.9168	3.23	833.01	2.80	1768.66	2.102
3600	0.4	0.33	0.99	3	48.3092	2.69	824.51	3.01	1842.16	2.345
3600	0.55	0.33	0.99	2	53.2725	2.18	928.76	2.23	2020.60	1.640
3600	0.55	0.35	0.99	1	52.5526	1.80	968.85	2.00	2079.86	1.634
3800	0.55	0.35	0.99	2	59.3724	1.82	1049.38	1.863	2162.30	0.881
3600	0.7	0.33	1.05	2	56.7721	2.03	961.93	1.99	1970.09	1.539
3600	0.55	0.33	1.05	3	51.1696	2.73	922.40	2.65	1922.04	1.997
3800	0.55	0.33	0.99	1	61.2423	1.72	1138.06	1.35	2223.30	0.800

- 0.00203625A*E + 24.5694B*C + 11.5488B*D - 0.373333B*E + 25.1778C*D -1.32747C*E - 2.58095D*E

For Lead:

MRR = -13961.9 + 5.73727A + 6875.08B - 2320.47C + 3365.86D + 607.050E - 5.96565e^{-04}A*A - 2790.52B*B - 25643.8C*C - 3056.18D*D - 16.5610E*E - 0.874956A*B + 1.62406A*C -0.375350A*D - 0.0577917A*E + 1746.43B*C - 720.343B*D - 105.858B*E + 14103.7C*D -681.392C*E - 114.871D*E

SR = - 45.9273 + 0.0396519A + 9.14096B - 120.471C - 10.1247D + 3.53665E - 6.23825e^{06} A*A + 5.22830B*B + 86.1907C*C + 1.20020D*D + 0.212358E*E - 0.00318333A*B + 0.0145270A*C + 9.23203e^{-05}A*D - 3.25000e^{-04}A*E - 19.2841B*C + 1.24719B*D + 0.183333B*E + 30.9078C*D - 4.44447C*E - 1.60457D*E

2.4 Prediction of MRR and SR Using ANFIS

The prediction of MRR and SR for all the three alloys using ANFIS is done by means of the Matlab software. The command used for ANFIS is ANFIS edit which displays a window as shown in Figure 3. Click the Load Date box in the window to enter the training data to display the training data plot in the ANFIS window as shown in Figure 4 and Figure 5 for MRR and SR respectively. After loading the training data, the user has to select the type of membership function and number of membership functions for each input. To generate (Fuzzy Inference System) FIS portion from ANFIS window, click on generate FIS. Now it is displayed to another window as shown in Figure 6. Select gauss2mf membership function from MF type to input and linear membership function to output. Assign three member ship functions for each input as shown in number of MFs. Close the window by selecting ok. Now select method and number of epochs from train FIS portion of ANFIS window. Then click on train now to train ANFIS with training data. After training was completed for 50 epochs, training curve will display as shown in Figure 7 and Figure 8 for MRR and SR respectively. This curve shows the reduction of error for each epoch, and it was observed in Figure 7 and 8. The curve reached the minimum error target and there was no further reduction of error possible. Now load the test data to ANFIS as a testing data, and select the testing data in test FIS portion of ANFIS window and click test now. Then two different types of points, square points (in blue color) which represents the experimental results and points (in red color) which represents the predicted outputs for given training data as shown in Figure 9 and Figure 10 for MRR and SR respectively. It can be observed from these Figures that all predicted outputs for testing data are very close to the experimental outputs of testing data. The predicted MRR and SR values are found in Ruler Viewer of ANFIS as shown in the Figures 11 and 12. The ANFIS model structure for five inputs and one output is shown

in Figure 13. This is the complete training and testing procedure of ANFIS for prediction of material removal rate and surface roughness. Figures 3 to 13 show all the steps in ANFIS for Copper Iron alloy. Similarly all the similar steps for Aluminium 6061 alloy and Lead tin alloy is done separately.

The comparison between predicted and experimental values of MRR and SR using ANFIS for Aluminium alloy is depicted in Figures 14 and 15. Table 3 shows that the predicted values are found very closer to the experimental values. It also shows the comparison of error

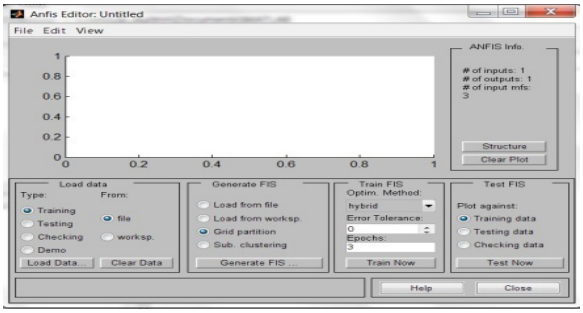

Figure 3. ANFIS Window in Matlab.

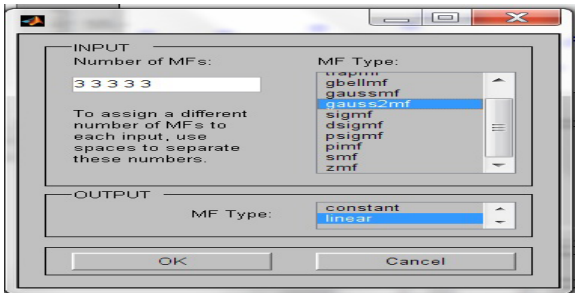

Figure 4. ANFIS Window after Loading MRR Training Data.

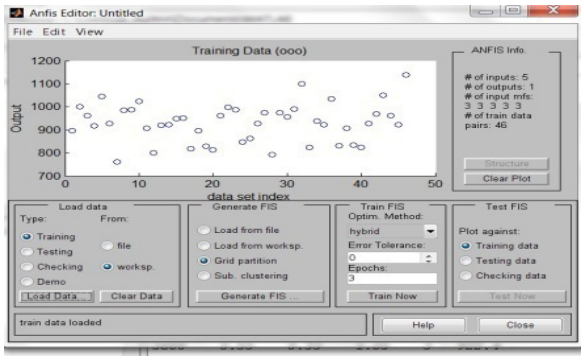

Figure 5. ANFIS Window after Loading SR Training Data (Cu).

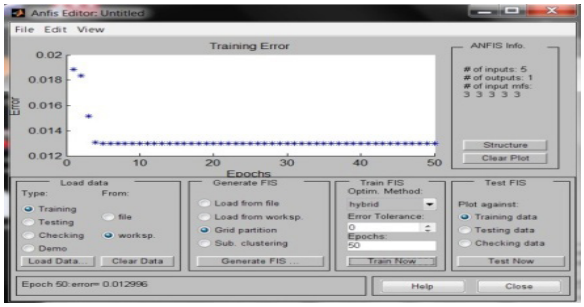

Figure 6. Generate FIS Window of ANFIS.

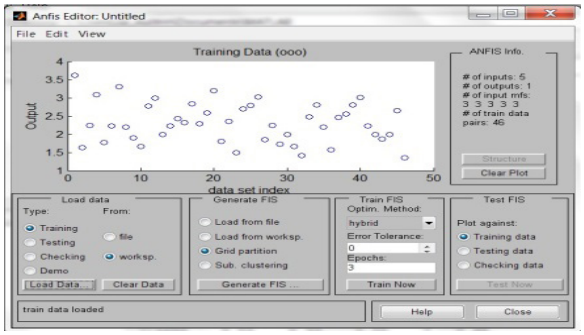

Figure 7. ANFIS Window after Training MRR Data (Cu).

Figure 8. ANFIS Window after Training SR Data (Cu).

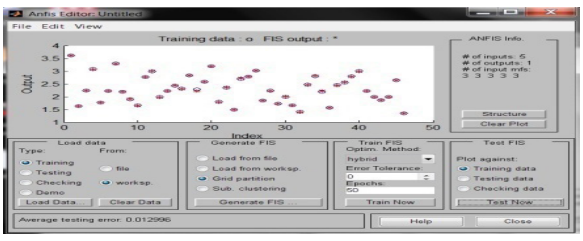

Figure 9. ANFIS window after Testing MRR Data (Cu).

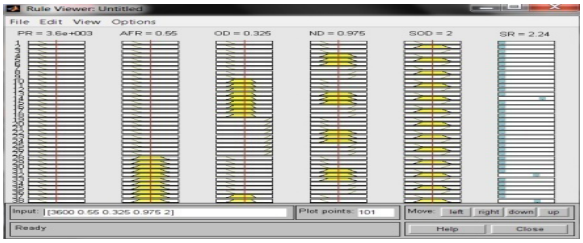

Figure 10. ANFIS Window after Testing SR Data (Cu).

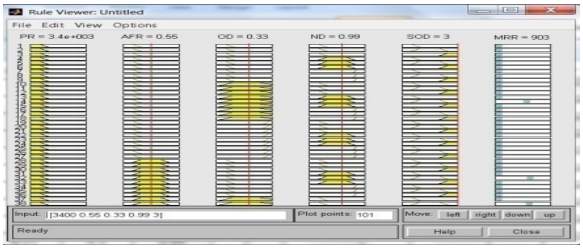

Figure 11. Rule Viewer for Predicted MRR Values (Cu).

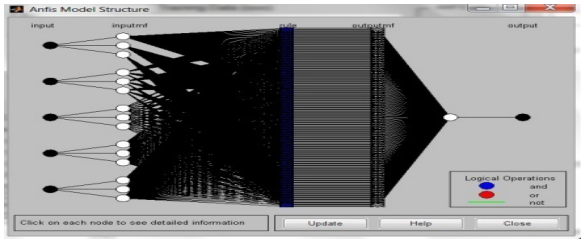

Figure 12 and 13. Rule Viewer for Predicted SR Values (Cu).

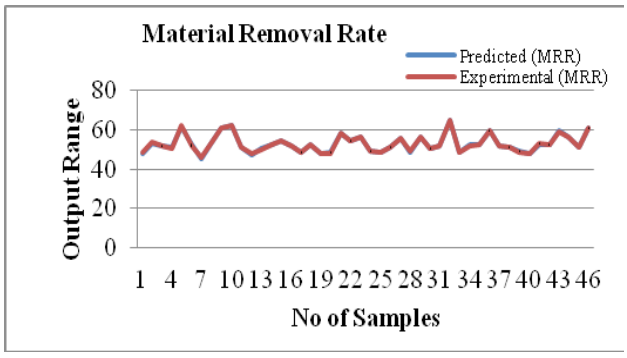

Figure 14. Comparisons of Predicted MRR and Experimental MRR (Al).

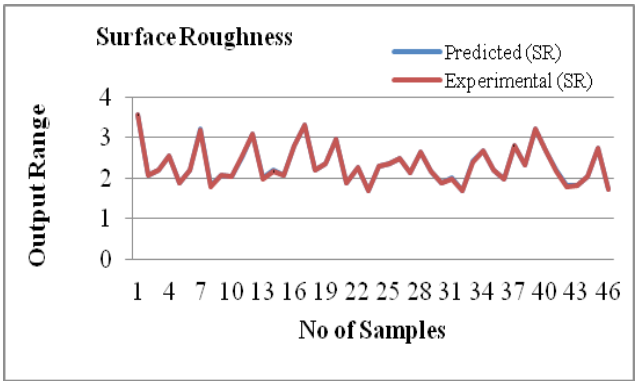

Figure 15. Comparisons of Predicted SR and Experimental SR (Al).

values for RSM and ANFIS and comparison of RSM and ANFIS Least Mean Square Error Values for MRR and SR which shows that the Error values and Least Mean Square Error for ANFIS is very less while compared to RSM for Aluminium alloy.

The comparison between predicted and experimental values of MRR and SR using ANFIS for copper alloy is depicted in Figures 16 and 17. Table 4 shows that the predicted values are found very closer to the experimental values. It also shows the comparison of error values for RSM and ANFIS and comparison of RSM and ANFIS Least Mean Square Error Values for MRR and SR which shows that the Error values and Least Mean Square Error for ANFIS is very less while compared to RSM for copper alloy.

The comparison between predicted and experimental values of MRR and SR using ANFIS for lead alloy is depicted in Figures 18 and 19. Table 5 shows that the predicted values are found very closer to the experimental values. It also shows the comparison of error values for RSM and ANFIS and comparison of RSM and ANFIS Least Mean Square Error Values for MRR and SR which shows that the Error values and Least Mean Square Error for ANFIS is very less while compared to RSM for lead alloy.

3. Results and Discussion

3.1 Effect of Process Parameters on Material Removal Rate for Aluminium 6061 Alloy

Figures 20 to 29 show the effects of input process parameters used in this study such as waterjet pressure, rate of abrasive flow, diameter of the orifice, diameter of the nozzle and stand of distance on the response MRR for cutting

Table 3. Comparison between the Error and Least Mean Square Error of RSM and ANFIS for MRR and SR for Aluminium 6061 Alloy

Sl. No.	Predicted MRR (mm3/min) Using ANFIS	Error MRR Using ANFIS	Error MRR Using RSM	Predicted SR (μm) Using ANFIS	Error SR Using ANFIS	Error SR Using RSM
1	48.1	1.051406	1.443585	3.56	0.28011	0.15964
2	53.4	0.447242	0.609506	2.08	0	1.72271
3	52.0	0.285621	1.113345	2.21	0	0.38539
4	51.1	0.520899	0.53218	2.54	0.39216	0.68585
5	61.9	0.517822	0.11579	1.89	0.52632	0.23761
6	52.8	1.828477	1.651953	2.19	0	0.20923
7	45.6	0.331355	0.139565	3.21	0.3125	0.65087
8	53.6	0.074385	1.410356	1.81	0.05556	1.38293
9	61.3	0.094216	0.918782	2.07	0	0.62955
10	62.1	0.196393	0.546128	2.05	0	1.98682
11	51.2	0.05941	1.233395	2.53	0.3937	0.08124
12	47.6	0.243941	1.4064	3.08	0	0.28142
13	50.4	0.440023	1.306339	2.00	0.50251	1.98073
14	52.8	0.208089	0.381082	2.19	0.92166	0.7105
15	54.3	0.165655	2.476147	2.08	0	1.69355
16	51.7	0.29295	0.490423	2.79	0	0.64989
17	48.7	0.18288	0.246409	3.30	0	0.27654
18	52.8	0.208089	0.381082	2.19	0	0.20923
19	47.9	0.384773	0.276932	2.36	0	0.46431
20	48.8	1.015956	0.784941	2.96	0.33898	1.39724
21	58.5	0.036766	0.762979	1.90	0.5291	1.56395
22	54.5	0.498602	0.693319	2.26	0.44444	1.16724
23	56.3	0.107699	0.628993	1.69	0.59524	0.05293
24	49.4	0.352656	0.708614	2.29	0	0.40076
25	48.9	0.034344	1.837778	2.36	0	0.47499
26	51.3	0.254839	0.841824	2.50	0	1.04148
27	55.9	0.09865	0.11053	2.14	0	0.42778
28	48.9	0.663059	0.030145	2.65	0	1.23968
29	56.6	0.303142	0.711547	2.18	0	0.53922
30	50.6	0.462672	0.856829	1.90	0	0.17781
31	51.9	0.092764	0.430451	2.00	0.50251	1.96228
32	64.9	0.131451	0.062823	1.70	0	0.70083
33	48.5	0.228549	0.592409	2.41	0.41667	0.3126
34	52.3	0.191763	0.020404	2.69	0.37313	0.48561
35	52.8	0.208089	0.381082	2.19	0.45455	0.66282
36	59.5	0.550067	0.640535	1.99	0	1.4636

Table 3. Comparison between the Error and Least Mean Square Error of RSM and ANFIS for MRR and SR for Aluminium 6061 Alloy

Sl. No.	Predicted MRR (mm3/min) Using ANFIS	Error MRR Using ANFIS	Error MRR Using RSM	Predicted SR (μm) Using ANFIS	Error SR Using ANFIS	Error SR Using RSM
37	51.9	0.092764	0.65866	2.81	0.35714	0.73733
38	51.6	0.841124	1.136787	2.34	0	0.02899
39	49.4	0.9878	1.484928	3.23	0	0.15912
40	48.3	0.019044	0.162944	2.68	0.37175	0.45591
41	52.8	0.886949	1.058765	2.19	0.45872	0.24853
42	52.9	0.661052	0.152343	1.81	0.55556	0.72328
43	59.5	0.214915	1.615305	1.81	0.54945	0.66866
44	56.7	0.126999	2.718975	2.03	0	1.13511
45	51.0	0.331447	0.685909	2.74	0.3663	1.1317
46	61.0	0.395642	0.202849	1.72	0	0.82097
Least Mean Square Error MRR for RSM					0.148249	
Least Mean Square Error MRR for ANFIS					0.075355	
Least Mean Square Error SR for RSM					0.137694	
Least Mean Square Error SR for ANFIS					0.047660	

Table 4. Comparison between the Error and Least Mean Square Error of RSM and ANFIS for MRR and SR for Copper Iron Alloy

Sl. No.	Predicted MRR (mm3/min) Using ANFIS	Error MRR Using ANFIS	Error MRR Using RSM	Predicted SR (μm) Using ANFIS	Error SR Using ANFIS	Error SR Using RSM
1	903	0.579193584	1.878906	3.62	0	0.18998
2	1000	0.002999910	0.291186	1.63	0	2.01916
3	963	0.111234705	2.467892	2.25	0.44643	1.80644
4	920	0.194944512	0.599156	3.08	0.32362	0.69508
5	1040	0.379324878	0.495263	1.77	0.16978	1.54915
6	921	0.835522632	1.116426	2.23	0.08977	0.35086
7	762	0.038043264	1.375882	3.29	0.57419	0.41846
8	987	0.163387085	1.718834	2.19	0	0.76341
9	990	0.222717149	0.931024	1.91	0.47344	1.66912
10	1020	0.527593841	1.163409	1.65	0.60241	0.9634
11	911	0.342552512	1.810896	2.77	0	0.40329
12	808	0.997475063	0.654059	3.01	0.63524	0.71371
13	925	0.510703032	0.380924	1.98	0.45249	1.16909

(*Continued*)

Table 4. Comparison between the Error and Least Mean Square Error of RSM and ANFIS for MRR and SR for Copper Iron Alloy (Continue)

Sl. No.	Predicted MRR (mm3/min) Using ANFIS	Error MRR Using ANFIS	Error MRR Using RSM	Predicted SR (μm) Using ANFIS	Error SR Using ANFIS	Error SR Using RSM
14	921	0.151777971	0.434618	2.23	0.26978	0.53135
15	946	0.250954259	0.136459	2.44	0.41152	2.87254
16	951	0.039973912	1.87803	2.31	0.43103	0.97746
17	819	0.141837034	1.232423	2.84	0.35336	0.91963
18	921	2.584094453	2.293505	2.23	2.62009	2.36606
19	829	0.134075783	2.87923	2.59	0.03862	0.15216
20	814	0.066295087	0.710342	3.19	0	0.35031
21	961	0.096680632	2.024162	1.78	1.05614	0.7779
22	999	0.144352219	0.073196	2.36	0.12728	0.77744
23	986	0.182223122	0.098441	1.5	0	2.10261
24	846	0.115705211	0.519132	2.72	0.74074	0.32983
25	858	0.610469494	0.097368	2.79	0	2.15337
26	927	0.189499978	0.497468	3.03	0	1.88193
27	974	0.049305613	0.209475	1.85	0	1.65886
28	796	0.482213638	0.45243	2.23	0.44643	0.73598
29	970	0.361574493	0.987546	1.73	0.23068	1.21237
30	964	0.692522222	0.499189	2.01	0.5	1.30556
31	997	0.68469633	0.548861	1.67	0.60241	2.10325
32	1100	0.077213063	0.057019	1.4	0.49751	1.22861
33	821	0.42570739	0.938293	2.47	0	0.11208
34	937	0.272467964	0.451911	2.82	0.71429	1.09195
35	921	0.151777971	0.434618	2.23	1.31758	1.58188
36	1040	0.392883689	0.205726	1.57	0.38363	1.4942
37	828	0.396968603	1.005071	2.45	0.2443	0.69785
38	909	0.122261507	0.716311	2.57	0.39062	0.27364
39	828	0.601433356	0.716609	2.79	0.35714	0.18289
40	826	0.180713393	0.395826	3	0.33223	2.42911
41	921	0.835522632	1.116426	2.23	0	0.26086
42	969	0.015482273	0.292896	2	0	2.06066
43	1050	0.059082506	0.300565	1.87	0.37574	2.29979
44	965	0.319150042	0.3552	1.99	0	2.07628
45	922	0.043365134	0.850008	2.66	0.37736	0.33818
46	1140	0.170465529	0.989072	1.35	0	0.61975
Least Mean Square Error MRR for RSM					0.161162	
Least Mean Square Error MRR for ANFIS					0.066068	
Least Mean Square Error SR for RSM					0.201764	
Least Mean Square Error SR for ANFIS					0.084770	

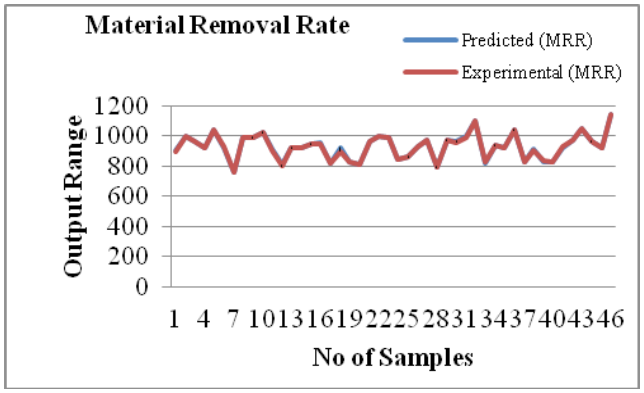

Figure 16. Comparisons of Predicted MRR and Experimental MRR (Cu).

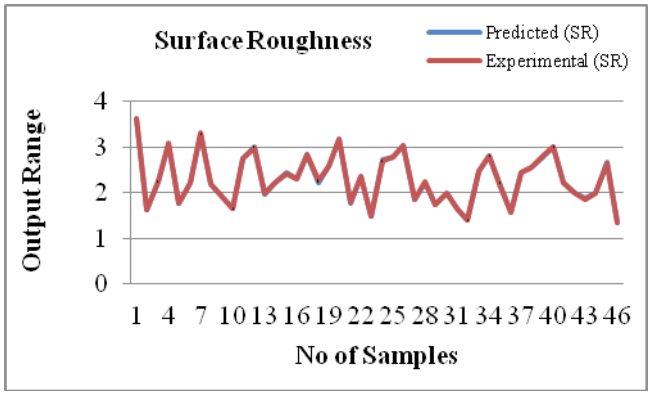

Figure 17. Comparisons of Predicted SR and Experimental SR (Cu).

Table 5. Comparison between the Error and Least Mean Square Error of RSM and ANFIS for MRR and SR for Lead Tin alloy

Sl. No.	Predicted MRR (mm3/min) Using ANFIS	Error MRR Using ANFIS	Error MRR Using RSM	Predicted SR (μm) Using ANFIS	Error SR Using ANFIS	Error SR Using RSM
1	1700	0.0266238	0.140804	2.44	0.40816	0.22129
2	2010	0.2412078	0.22388	1.41	0.35336	1.64361
3	1970	0.0045683	1.455883	1.63	0.36946	1.3945
4	1910	0.3573571	0.255508	2.2	0	0.18168
5	2190	0.3546782	0.698198	0.786	0.25381	1.20364
6	2010	0.6086574	0.419778	1.6	0.55935	0.60723
7	1690	0.0799455	2.564097	2.1	0.42674	0.86209
8	2000	0.1081168	0.50632	1.52	0	1.95643
9	2090	0.1927152	0.293584	1.2	0.08326	0.16391
10	2140	0.427603	0.120616	0.805	0.49938	1.39366
11	1890	0.3343282	1.543912	2.1	0	1.27126
12	1750	0.1786041	1.521448	1.9	0.26247	1.01542
13	1940	0.1600527	0.727295	1.88	0.37096	0.40004
14	2010	0.0418085	0.146007	1.6	1.84596	1.79693
15	1940	0.4331671	0.070388	1.54	0.65359	2.00431
16	2010	0.3254338	0.554358	1.71	0.05851	2.52001
17	1740	0.0389941	0.085287	1.9	0	0.34481
18	2010	0.3254338	0.137086	1.6	2.17114	2.12195
19	1840	0.1172537	1.907532	1.91	0	0.14304
20	1760	0.5030865	0.899159	1.89	0.47393	1.09612
21	2130	0.2925688	1.619043	1.2	0.90834	0.36569
22	1900	0.4605322	0.091595	1.98	0.95048	0.9955
23	2070	0.6931777	0.139848	1.42	0.76869	0.66169

(*Continued*)

Table 5. Comparison between the Error and Least Mean Square Error of RSM and ANFIS for MRR and SR for Lead Tin alloy

Sl. No.	Predicted MRR (mm3/min) Using ANFIS	Error MRR Using ANFIS	Error MRR Using RSM	Predicted SR (μm) Using ANFIS	Error SR Using ANFIS	Error SR Using RSM
24	1860	0.3429061	1.002258	2.01	0.14903	0.39509
25	1840	0.1172537	1.166095	1.94	0.25707	1.30973
26	1920	0.1643321	0.62	2.01	0.0996	0.35867
27	1970	0.0045683	0.260923	1.5	0	0.88189
28	1790	0.0599751	0.905793	1.78	0.50307	0.12
29	1940	0.1135308	0.82164	1.7	0.05886	0.69401
30	2040	0.4785809	0.03452	1.71	0.17575	2.39642
31	2010	0.0418085	0.190011	1.5	0	0.02388
32	2140	0.1255431	0.064608	0.615	0.80645	0.56586
33	1860	0.3429061	1.390375	1.94	0.31024	0.4587
34	1910	0.3568373	0.067327	2.31	0.04331	0.83406
35	2010	0.2412078	0.428492	1.6	0.18785	0.13962
36	2170	0.0561023	0.275813	0.798	0.25	1.86871
37	1800	0.0044443	0.56061	1.89	0.52632	1.00533
38	2020	0.0296942	0.790682	1.71	0.35211	0.99448
39	1770	0.0757636	0.361177	2.09	0.57088	1.24783
40	1840	0.1172537	0.516789	2.36	0.63966	0.76675
41	2010	0.5245967	0.711348	1.6	2.43902	2.48599
42	2080	0.0067312	0.939652	1.64	0.3672	2.17561
43	2170	0.3561023	0.991671	0.878	0.34052	0.20328
44	1970	0.0045683	0.072769	1.54	0.06498	0.61716
45	1920	0.1061372	0.770923	2	0.15023	0.00119
46	2220	0.148428	0.900289	0.801	0.125	1.19214
Least Mean Square Error MRR for RSM					0.12714	
Least Mean Square Error MRR for ANFIS					0.041937	
Least Mean Square Error SR for RSM					0.178674	
Least Mean Square Error SR for ANFIS					0.099991	

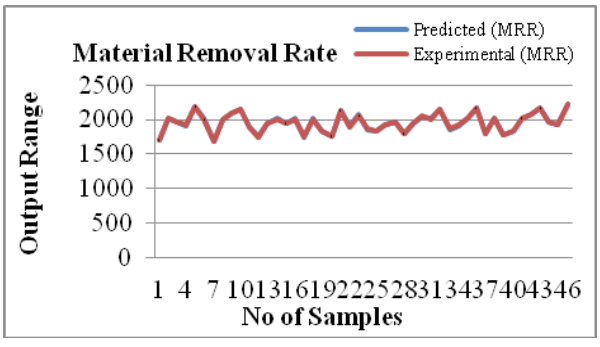

Figure 18. Comparisons of Predicted MRR and Experimental MRR (Pb).

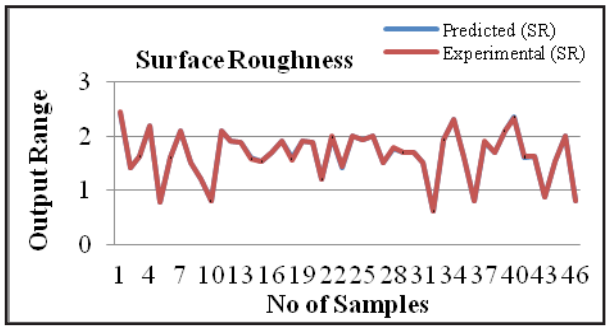

Figure 19. Comparisons of Predicted SR and Experimental SR (Pb).

Aluminium 6061 alloy using AWJM. Figures 20-23 illustrate that as the pressure of the abrasive water jet increases, rate of abrasive flow increases, diameter of the orifice decreases, diameter of the nozzle decreases and standoff distance decreases, MRR increases due to the high pressure, minor diameter of orifice and nozzle increases the velocity of water jet when impinged on the work surface with low standoff distance. Figures 24–26 illustrate that as the abrasive flow rate increases the MRR also increases due to the rate of flow of the abrasives and water increases. Figures 27–29 illustrate as the diameter of orifice and nozzle decreases produce high MRR with low stand of distance. Thus when the pressure is 3800 bar, abrasive flow rate is 0.7Kg/min, Orifice diameter is 0.3mm, nozzle diameter is 0.9mm and standoff distance is 1mm, the MRR is high.

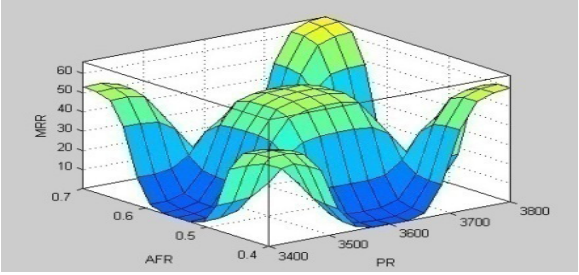

Figure 20. MRR vs. Pressure and Abrasive Flow Rate.

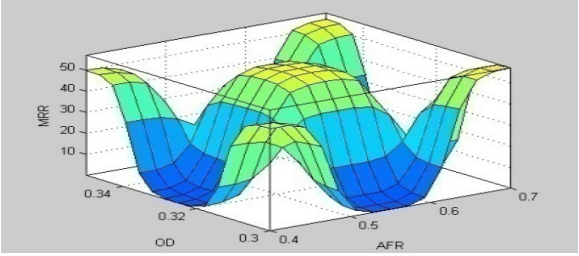

Figure 21. MRR vs. Pressure and Orifice Diameter.

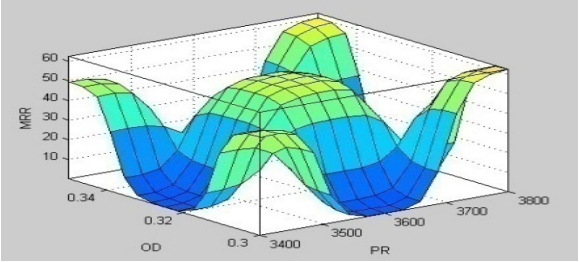

Figure 22. MRR vs. Pressure and Nozzle Diameter.

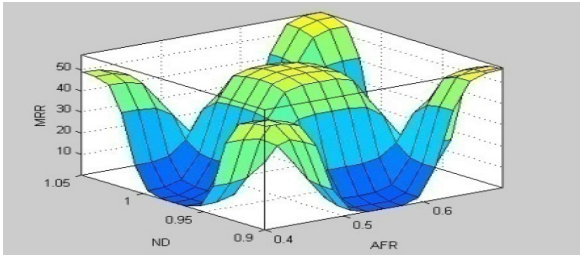

Figure 23. MRR vs. Pressure and Stand Off Distance.

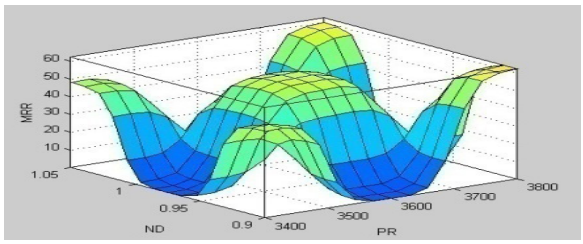

Figure 24. MRR vs. Abrasive Flow Rate and Orifice Diameter.

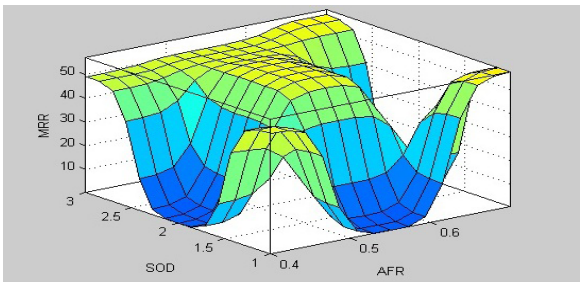

Figure 25. MRR vs. Abrasive Flow Rate and Nozzle Diameter.

3.2 Effect of Process Parameters on Surface Roughness for Aluminium 6061 Alloy

Figures 30 to 39 show the effects of input process parameters used in this study such as abrasive water jet pressure, rate of abrasive flow, diameter of orifice, diameter of nozzle and stand of distance on the response SR for cutting Aluminium 6061 alloy using AWJM. Figures 30-33 illustrate that as the pressure of the abrasive water jet increases, rate of abrasive flow increases, diameter of orifice decreases, diameter of nozzle decreases and standoff distance decreases produce good SR due to the high pressure, minor diameter of orifice and nozzle increases the velocity of water jet when impinged on the work surface

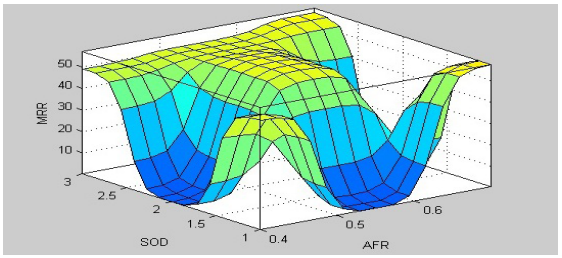

Figure 26. MRR vs. Abrasive Flow Rate and Stand Off Distance.

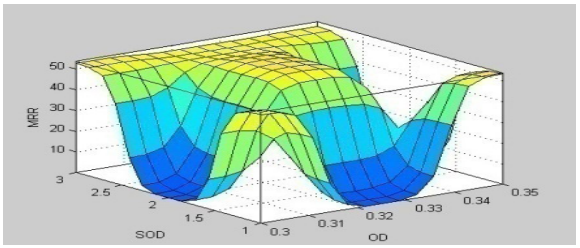

Figure 27. MRR vs. Orifice Diameter and Nozzle Diameter.

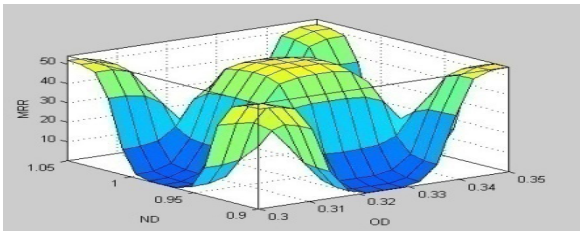

Figure 28. MRR vs. Orifice Diameter and Stand Off Distance.

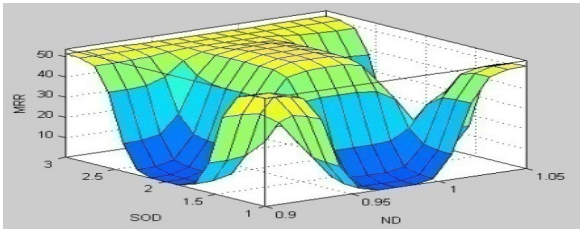

Figure 29. MRR vs. Nozzle Diameter and Stand Off Distance.

with low standoff distance. Figures 34-36 illustrate that as the abrasive flow rate decreases the SR value i.e, good surface finish also increases due to the rate of flow of the abrasives and water increases. Figures 37-39 illustrate as the diameter of orifice and nozzle decreases; it produces good SR with low stand of distance. Thus when the pressure is 3800 bar, abrasive flow rate is 0.7Kg/min, Orifice diameter is 0.3mm, nozzle diameter is 0.9mm and stand-off distance is 1mm, the SR obtained is very good.

3.3 Effect of Process Parameters on Material

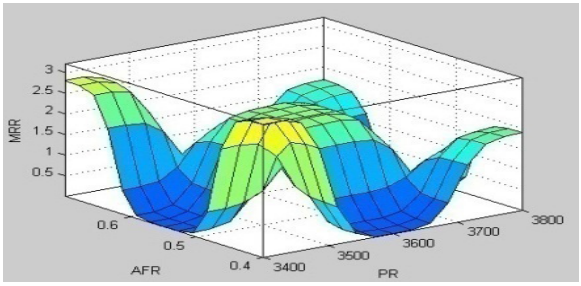

Figure 30. SR vs. Pressure and Abrasive Flow Rate.

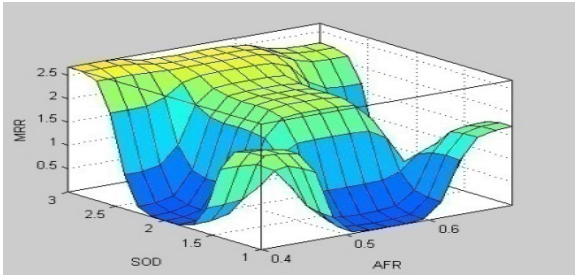

Figure 31. SR vs. Pressure and Orifice Diameter.

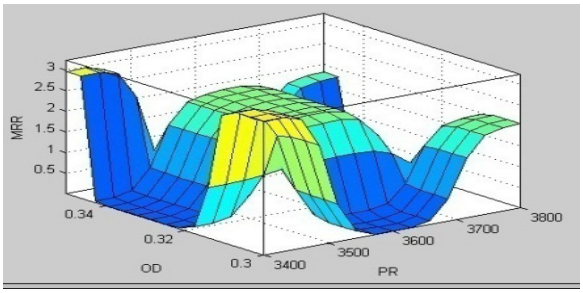

Figure 32. SR vs. Pressure and Nozzle Diameter.

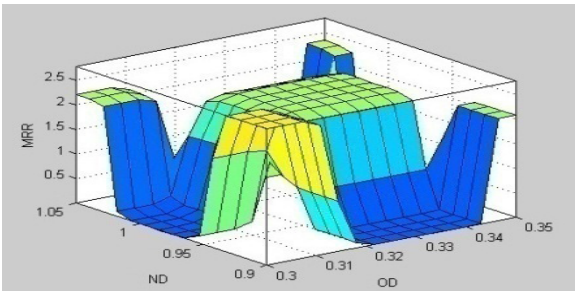

Figure 33. SR vs. Pressure and Stand Off Distance.

Removal Rate for Copper Iron Alloy

From Figures 40 to 49 the effects of input process parameters used in this study such as water jet pressure, rate of abrasive flow, diameter of orifice, diameter of nozzle and stand of distance on the response Material removal rate for cutting Copper iron alloy using AWJM is shown. The Figures 40-43 illustrates that as the pressure of the abrasive water jet increases, rate of abrasive flow increases, diameter of orifice decreases, diameter of nozzle decreases and standoff distance decreases the MRR increases due to the high pressure, minor diameter of orifice and nozzle increases the velocity of water jet when impinged on the work surface with low standoff distance. The Figure s 44-46 illustrates that as the abrasive flow rate increases the MRR also increases due to the rate of flow of the abrasives and water increases. Figures 47-49 illustrates as the diameter of orifice and nozzle decreases produce high MRR with low stand of distance. Thus when the pressure is 3800 bar, abrasive flow rate is 0.7 Kg/min, Orifice diameter is 0.3mm, nozzle diameter is 0.9mm and standoff distance is 1mm, the MRR is high.

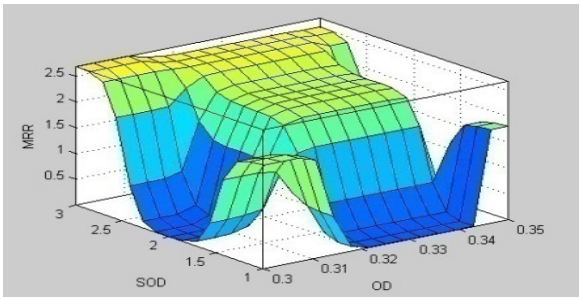

Figure 34. SR vs. Abrasive Flow Rate and Orifice Diameter.

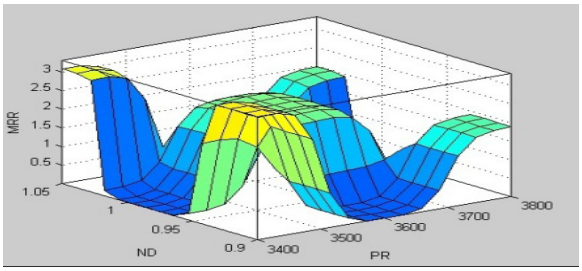

Figure 35. SR vs. Abrasive Flow Rate and Nozzle Diameter.

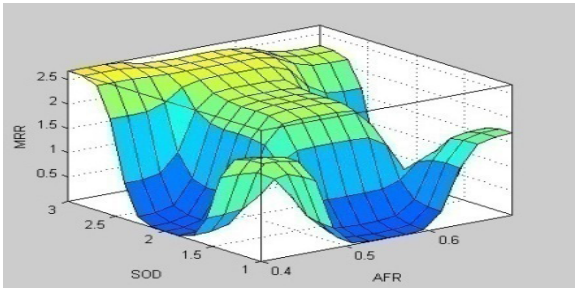

Figure 36. SR vs. Abrasive Flow Rate and Stand off Distance.

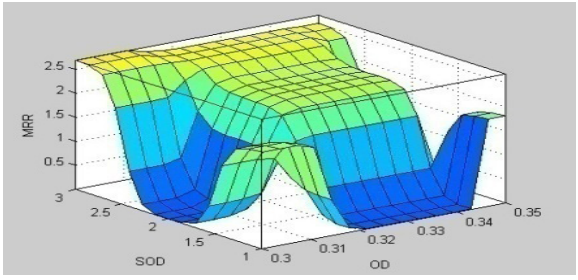

Figure 37. SR vs. Orifice Diameter and Nozzle Diameter.

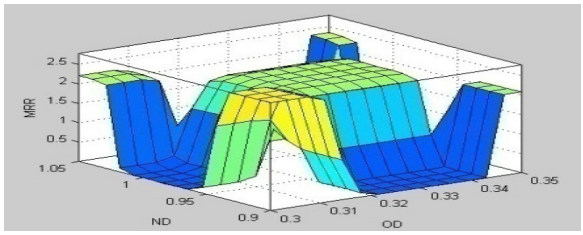

Figure 38. SR vs. Orifice Diameter and Stand Off Distance.

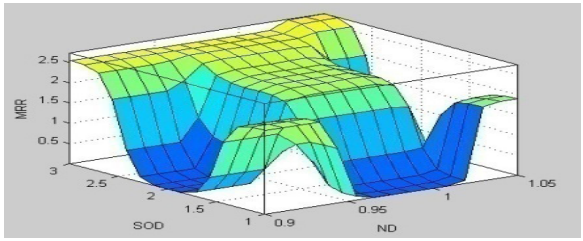

Figure 39. SR vs. Nozzle Diameter and Stand Off Distance.

3.4 Effect of Process Parameters on SR for Copper Iron Alloy

Figures 50 to 59 show the effects of input process parameters used in this study such as water jet pressure, rate of abrasive flow, diameter of orifice, diameter of nozzle and stand of distance on the response Surface Roughness for cutting Copper Iron alloy using AWJM. The Figures 50-53 illustrate that as the pressure of the abrasive water jet increases, rate of abrasive flow increases, diameter of

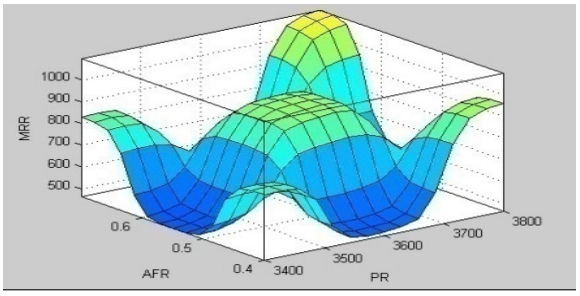

Figure 40. MRR vs. Pressure and Abrasive Flow Rate.

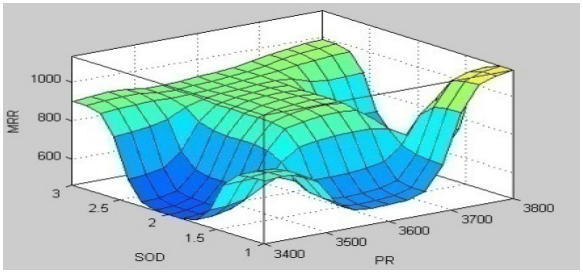

Figure 41. MRR vs. Pressure and Orifice Diameter.

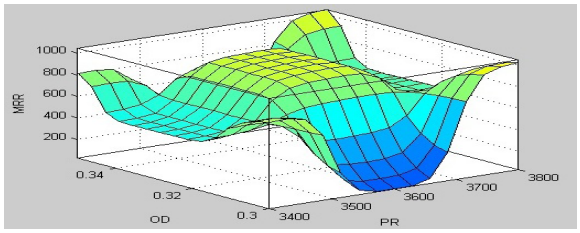

Figure 42. MRR vs. Pressure and Nozzle Diameter.

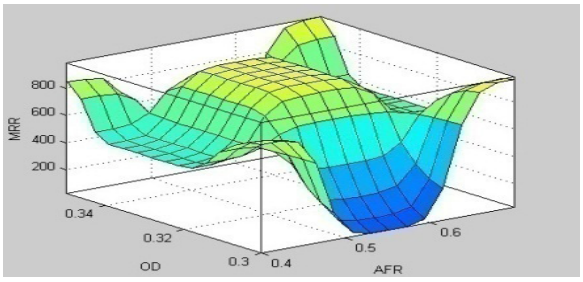

Figure 43. MRR vs. Pressure and Stand Off Distance.

orifice decreases, diameter of nozzle decreases and stand-off distance decreases produce good SR due to the high pressure, minor diameter of orifice and nozzle increases the velocity of water jet when impinged on the work surface with low standoff distance. The Figures 54-56 illustrate that as the abrasive flow rate decreases the SR

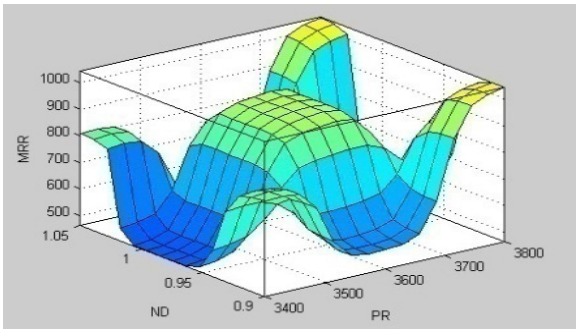

Figure 44. MRR vs. Abrasive Flow Rate and Orifice Diameter.

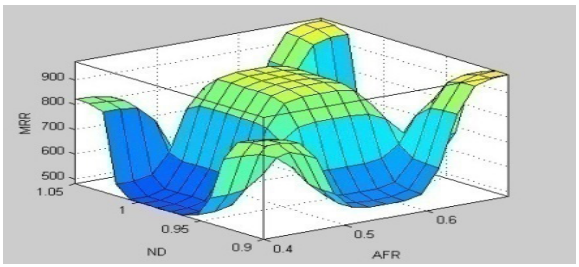

Figure 45. MRR vs. Abrasive Flow Rate and Nozzle Diameter.

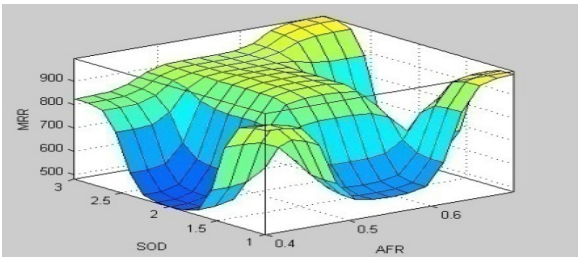

Figure 46. MRR vs. Abrasive Flow Rate and Stand Off Distance.

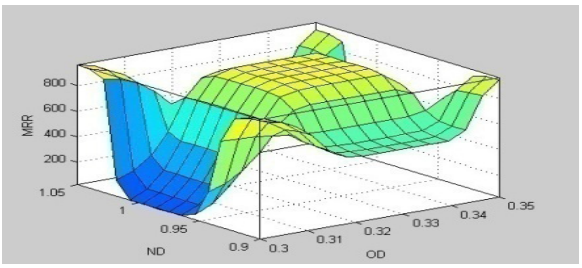

Figure 47. MRR vs. Orifice Diameter and Nozzle Diameter.

value i.e., good surface finish also increases due to the rate of flow of the abrasives and water increases. Figures 57-59 illustrate as the diameter of orifice and nozzle decreases produce good SR with low stand of distance. Thus when

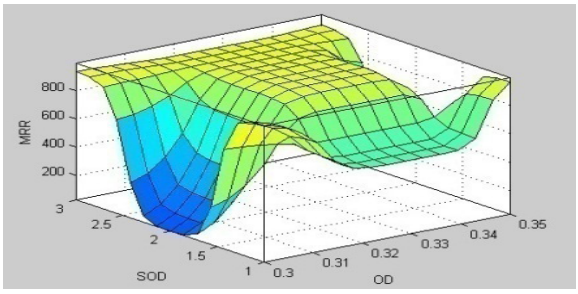

Figure 48. MRR vs. Orifice Diameter and Stand Off Distance.

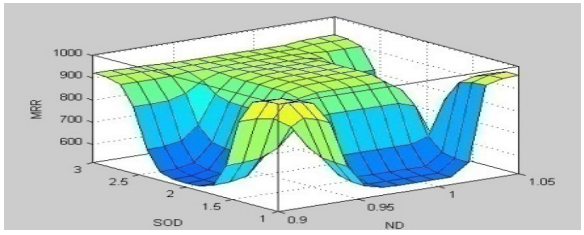

Figure 49. MRR vs. Nozzle Diameter and Stand Off Distance.

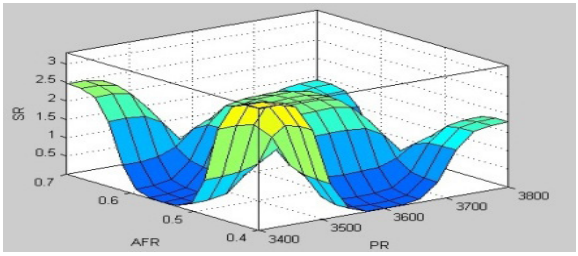

Figure 50. SR vs. Pressure and Abrasive Flow Rate.

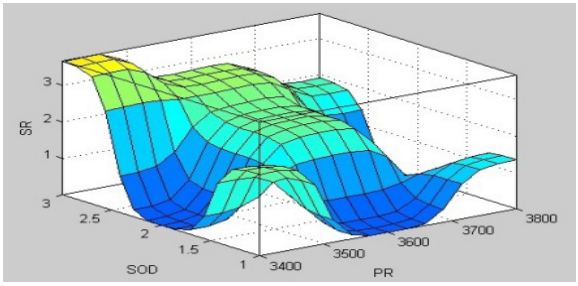

Figure 51. SR vs. Pressure and Orifice Diameter.

the pressure is 3800 bar, abrasive flow rate is 0.7Kg/min, Orifice diameter is 0.3mm, nozzle diameter is 0.9mm and standoff distance is 1mm, the SR obtained is good.

3.5 Effect of Process Parameters on Material

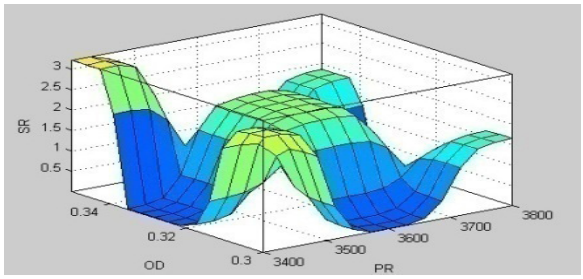

Figure 52. SR vs. Pressure and Nozzle Diameter.

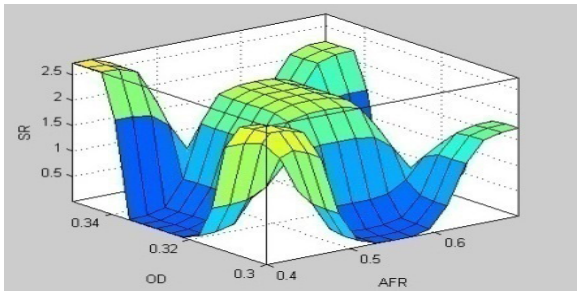

Figure 53. SR vs. Pressure and Stand Off Distance.

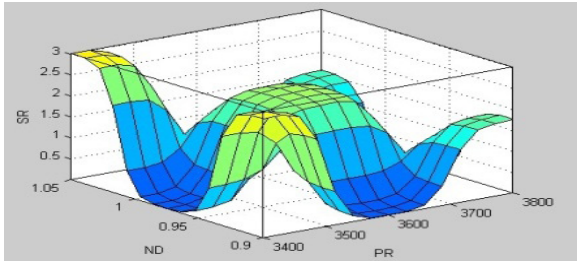

Figure 54. SR vs. Abrasive Flow Rate and Orifice Diameter.

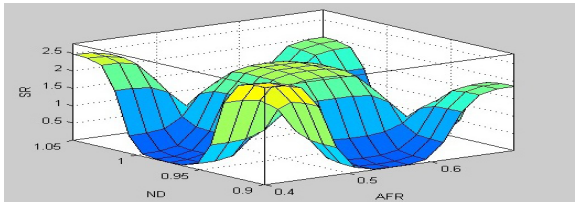

Figure 55. SR vs. Abrasive Flow Rate and Nozzle Diameter.

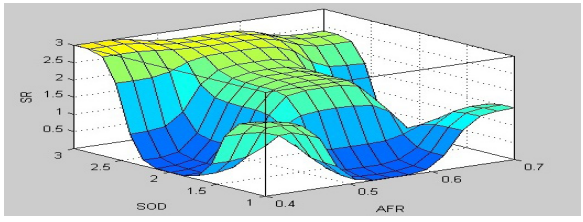

Figure 56. SR vs. Abrasive Flow Rate and Stand Off Distance.

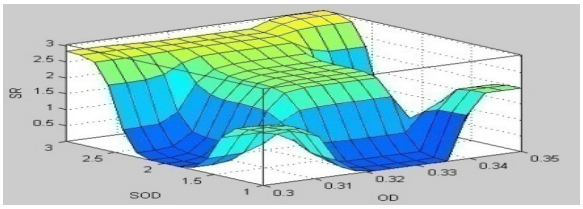

Figure 57. SR vs. Orifice Diameter and Nozzle Diameter.

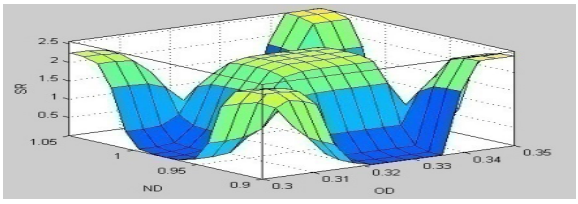

Figure 58. SR vs. Orifice Diameter and Stand Off Distance.

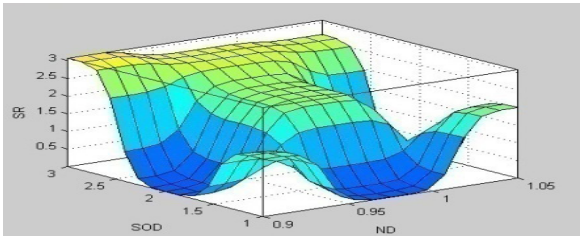

Figure 59. SR vs. Nozzle Diameter and Stand Off Distance.

Removal Rate for Lead Tin Alloy

Figures 60 to 69 show the effects of input process parameters used in this study such as abrasive water jet pressure, rate of abrasive flow, diameter of orifice, diameter of nozzle and stand of distance on the response MRR for cutting Lead Tin alloy using AWJM. Figures 60-63 illustrate that as the pressure of the abrasive water jet increases, rate of abrasive flow increases, diameter of orifice decreases, diameter of nozzle decreases and standoff distance decreases the MRR increases due to the high pressure, minor diameter of orifice and nozzle increases the velocity of water jet when impinged on the work surface with low standoff distance. Figures 64-66 illustrate that as the abrasive flow rate increases the MRR also increases due to the rate of flow of the abrasives and water increases. Figures 67-69 illustrate as the diameter of orifice and nozzle decreases produce high MRR with low stand of distance. Thus when the pressure is 3800 bar, abrasive flow rate is 0.7 Kg/min, Orifice diameter is 0.3mm, noz-

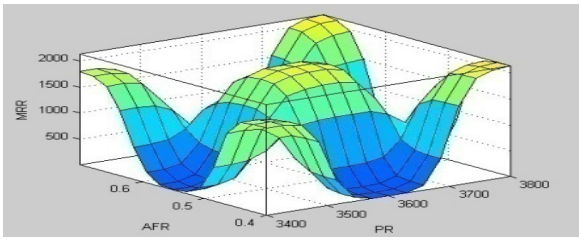

Figure 60. MRR vs. Pressure and Abrasive Flow Rate.

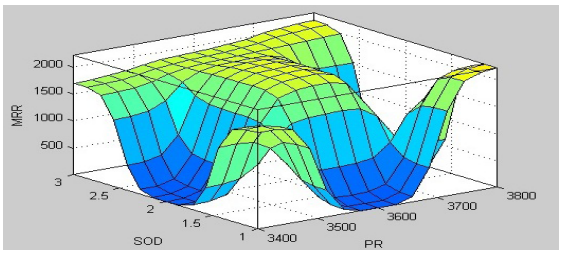

Figure 61. MRR vs. Pressure and Orifice Diameter.

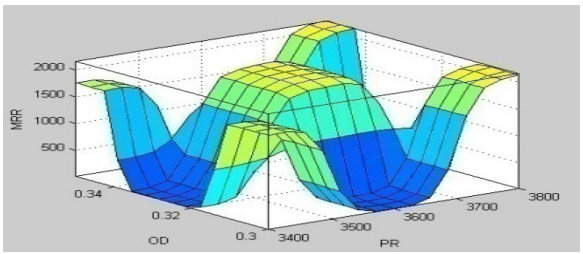

Figure 62. MRR vs. Pressure and Nozzle Diameter.

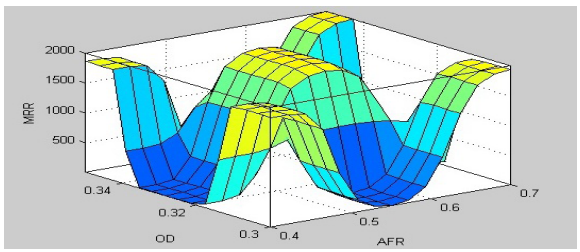

Figure 63. MRR vs. Pressure and Stand Off Distance.

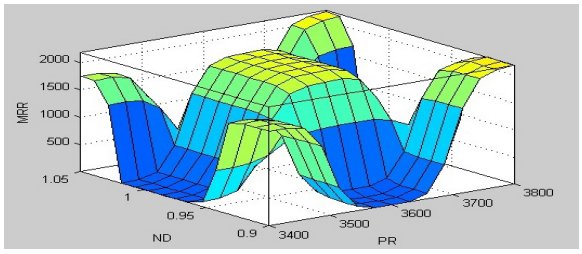

Figure 64. MRR vs. Abrasive Flow Rate and Orifice Diameter.

zle diameter is 0.9mm and standoff distance is 1mm, the MRR is high.

3.6 Effect of Process Parameters on Surface

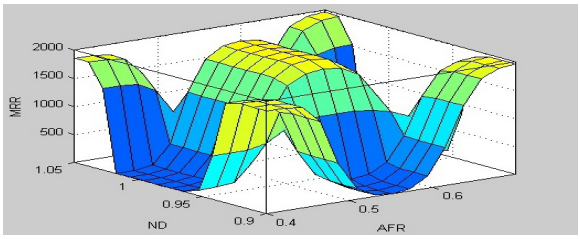

Figure 65. MRR vs. Abrasive Flow Rate and Nozzle Diameter.

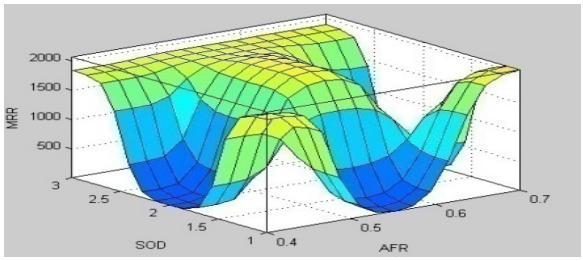

Figure 66. MRR vs. Abrasive Flow Rate and Stand Off Distance.

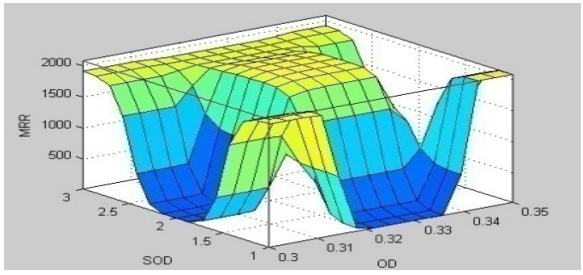

Figure 67. MRR vs. Orifice Diameter and Nozzle Diameter.

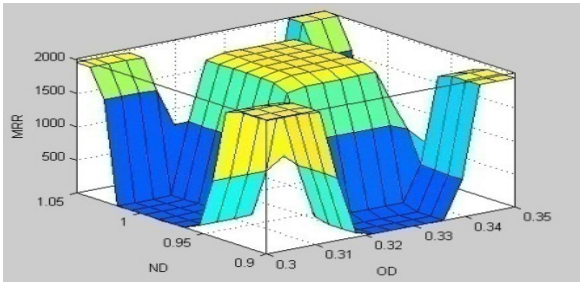

Figure 68. MRR vs. Orifice Diameter and Stand Off Distance.

Roughness for Lead Tin Alloy

From Figures 70 to 79 the effects of input process parameters used in this study such as abrasive water jet pressure, rate of abrasive flow, diameter of orifice, diameter of nozzle and stand of distance on the response Surface Roughness for cutting Lead Tin alloy using AWJM is shown. The Figures 70-73 illustrates that as the pressure of the abrasive water jet increases, rate of abrasive flow increases, diameter of orifice decreases, diameter of nozzle decreases and standoff distance decreases produce good surface roughness due to the high pressure, minor diameter of orifice and nozzle increases the velocity of water jet when impinged on the work surface with low standoff distance. Figures 74-76 illustrate that as the abrasive flow

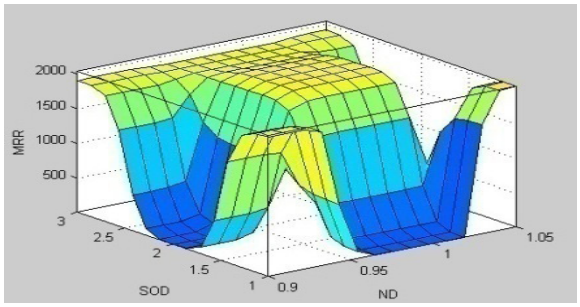

Figure 69. MRR vs. Nozzle Diameter and Stand Off Distance.

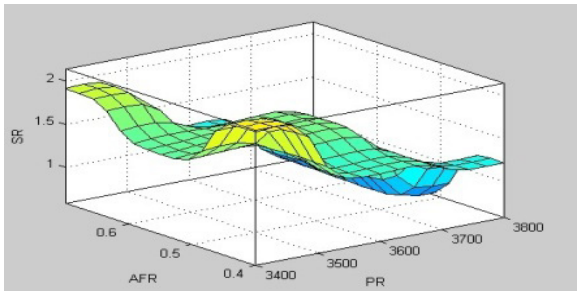

Figure 70. SR vs. Pressure and Abrasive Flow Rate.

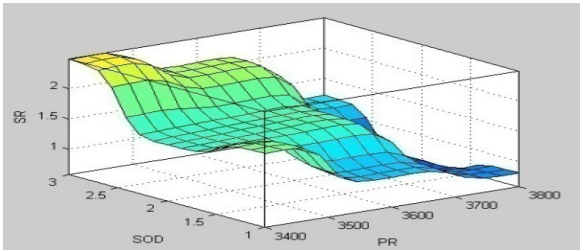

Figure 71. SR vs. Pressure and Orifice Diameter.

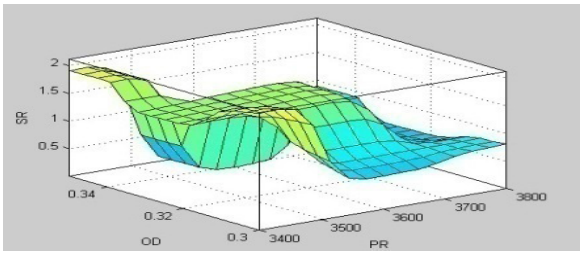

Figure 72. SR vs. Pressure and Nozzle Diameter.

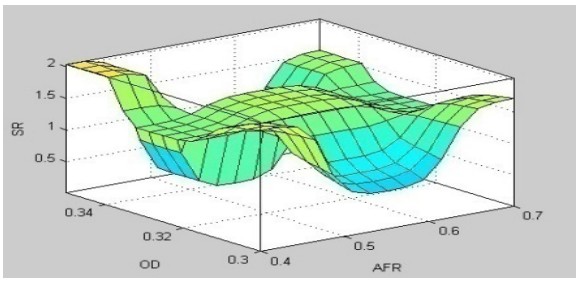

Figure 73. SR vs. Pressure and Stand Off Distance.

rate decreases the SR value i.e., good surface finish also increases due to the rate of flow of the abrasives and water increases. Figures 77-79 illustrate as the diameter of orifice and nozzle decreases produce good SR with low stand of distance. Thus when the pressure is 3800 bar, abrasive flow rate is 0.7Kg/min, Orifice diameter is 0.3mm, nozzle

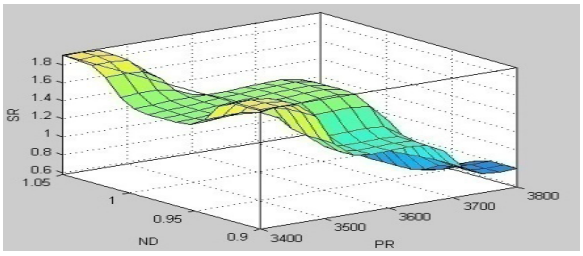

Figure 74. SR vs. Abrasive Flow Rate and Orifice Diameter.

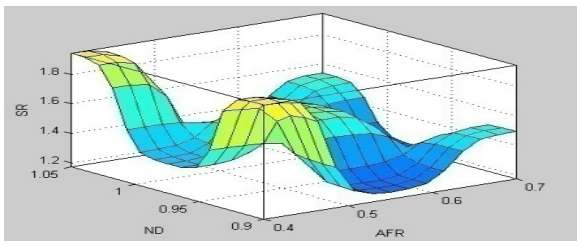

Figure 75. SR vs. Abrasive Flow Rate and Nozzle Diameter.

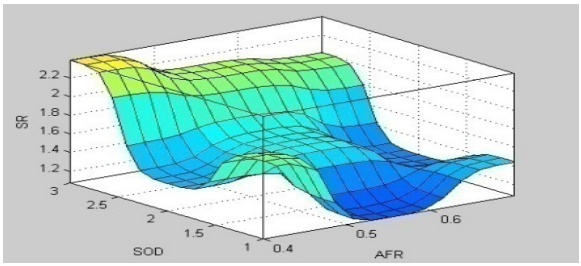

Figure 76. SR vs. Abrasive Flow Rate and Stand Off Distance.

diameter is 0.9mm and standoff distance is 1mm, the SR obtained is high.

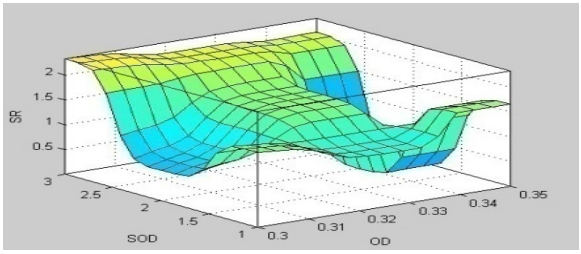

Figure 77. SR vs. Orifice Diameter and Nozzle Diameter.

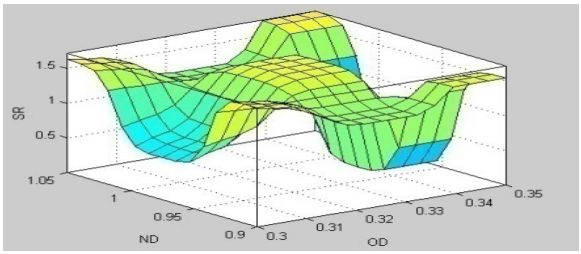

Figure 78. SR vs. Orifice Diameter and Stand Off Distance.

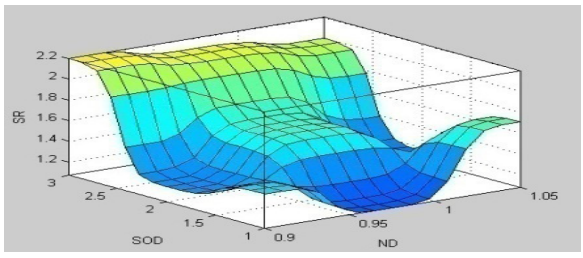

Figure 79. SR vs. Nozzle Diameter and Stand Off Distance.

4. Conclusion

In this paper, using linear regression analysis a mathematical model is developed for three nonferrous alloys through AWJM process by Minitab software is done. Then the prediction of MRR and SR for Aluminium 6061 alloy, Copper Iron alloy and Lead Tin alloy by cutting through AWJM process by the tool named ANFIS is done which illustrates that the experimental values are closer to the predicted values for all the three materials. The error comparison between RSM and ANFIS is also studied which shows the percentage of error is very less in ANFIS while compared with RSM. More over the effect of abrasive water jet pressure, rate of abrasive flow, diameter of orifice, diameter of focusing nozzle and standoff distance on MRR and SR is studied through this intelligent tool.

5. References

1. Abdel-Rahman AA. A Closed-Form Expression for an Abrasive Water Jet Cutting Model for Ceramic Materials. International Journal of Mathematical Models and Methods in Applied Sciences. 2011; 4(5):722–9.
2. Ma C, Deam RT. A Correlation for Predicting the Kerf Profile from AWJC. Experimental Thermal and Fluid Science. 2006; 30(4):337–43.
3. Liu H, Wang J, Kelson N, Brown RJ. Study of Abrasive Water Jet Characteristics by CFD Simulation. Journal of Materials Processing Technology. 2004; 153(1):488–93.
4. Suganthi XH, Natarajan U, Sathiyamurthy S, Chidambaram K. Prediction of Quality Responses in Micro-EDM Process Using an Adaptive Neuro-Fuzzy Inference System (ANFIS) Model. International Journal of Advanced Manufacturing Technology. 2013; 68(1):339–47.
5. Caydas U, Hascalik A, Ekici S. An Adaptive Neuro-Fuzzy Inference System (ANFIS) Model for Wire-EDM. Expert Systems with Applications. 2009; 36(3):6135–9.
6. Jang JSR. ANFIS: Adaptive Network Based Fuzzy Inference System. IEEE Transactions on Systems. Man Cybernetics. 1993; 23(3):665–85.
7. Yeh FH, Lu Y-H, Li C-L, Wu M-T. Application of ANFIS for Inverse Prediction of Hole Profile in the Square Hole Bore-Expanding Process. Journal of Materials Processing Technology. 2006; 173(2):136–44.
8. Reddy CB, Reddy VD, Reddy CE. Experimental Investigations on MRR and Surface Roughness of EN 19 & SS 420 Steels in Wire-EDM Using Taguchi Method. International Journal of Engineering Science and Technology. 2012; 4(11):4603–14.
9. Kolahan F, Khajavi AH. Statistical Approach for Predicting and Optimizing Depth of Cut in AWJ Machining for 6063-T6 Al Alloy. International Journal of Mechanical Systems Engineering. 2010; 2(2):143–6.
10. Wang J, Wong WCK. A Study of Abrasive Water Jet Cutting of Metallic Coated Sheet Steels. International Journal of Machine Tools and Manufacture. 1999; 39(6):855–70.
11. Nithyanandam J, Das SL, Palanikumar K. Influence of Cutting Parameters in Machining of Titanium Alloy. Indian Journal of Science and Technology. 2015 Apr; 8(S8):556–62.